ISSN 1063-7842, Technical Physics, 2020, Vol. 65, No. 11, pp. 1755–1759. © Pleiades Publishing, Ltd., 2020.
Russian Text © The Author(s), 2020, published in Zhurnal Tekhnicheskoi Fiziki, 2020, Vol. 90, No. 11, pp. 1838–1842.

SOLID STATE

Experimental Determination of mechanical Properties of the Anode Cell of an X-Ray Lithograph

N. A. Djuzhev[a],*, E. E. Gusev[a], A. A. Dedkova[a], D. A. Tovarnov[a], and M. A. Makhiboroda[a]
[a]*National Research University "MIET," Moscow, 124498 Russia*
**e-mail: bubbledouble@mail.ru*
Received April 2, 2020; revised April 2, 2020; accepted April 2, 2020

Abstract—We have prepared the anode cell of an X-ray lithograph in the form of a PolySi/Si_3N_4/SiO_2 membrane structure using group technology. The design of the stand for determining mechanical properties of membranes has been modernized. The critical pressure of a membrane structure with a diameter 250 μm varies in the range from 0.484 to 0.56 MPa for 15 samples. The mechanical strength of the PolySi*/Si_3N_4/SiO_2 structure is 3.13 GPa. The new model in the Comsol package shows good correlation between the experimental critical pressure and the theoretical mechanical strength of the membrane. The distribution of mechanical stresses over the membrane has been obtained by simulation and analytic calculation. It is proved that the structure breaking region is localized at the membrane/substrate interface.

DOI: 10.1134/S1063784220110055

INTRODUCTION

The tenfold exceedance of the diffraction limit of a lithograph working wavelength of 193 nm increases the cost of the process and equipment [1]. The version with projection photolithography in the extreme ultraviolet range (EUV lithography) with a working wavelength of 13.5 nm [2] used for the formation of critical chip sizes is insufficiently productive. One possible solution is maskless X-ray nanolithography [3], which potentially ensures efficient production. As a source of X-ray radiation in a lithograph, an X-ray tube including a cathode and a shot anode can be considered. This study is devoted to analysis of mechanical properties of a shooting anode cell (Fig. 1). The anode cell must withstand the vacuum atmosphere (excess pressure of 0.1 MPa) of the X-ray tube and possess sufficiently high X-ray transparency because of the small thickness of the material in the membrane region. As the element of the target, we chose polysilicon material, which makes it possible to generate a wave with a length of 13.5 nm. The SiO_2 and Si_3N_4 layers possess compressive and tensile stresses, which leads to compensation of stresses and increases the mechanical strength margin.

One problem in the development of silicon-based electronic devices is the reliability of information on mechanical properties of materials [4], especially on account of the size effect between bulk and film materials [5].

Therefore, it is necessary to perfect the metrological base of measurements. In [6], the mechanical strength of borosilicate glass was measured by the shock compression method. In [7], the mechanical strength of a gallium nitride layer formed using hydride-chloride vapor-phase epitaxy was determined with the help of an indenter. In our study, we used a contactless method of blowing a thin film with the help of excess pressure. An advantage of this method is the absence of introduced defects.

At present, technological approached to increasing the mechanical strength are being perfected. For example, circular membranes are used instead of rectangular ones [8]. This is because membrane rupture mainly occurs over the membrane–substrate inter-

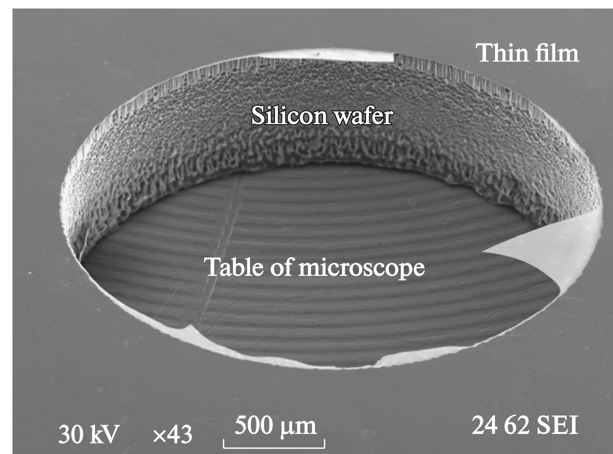

Fig. 1. Insufficient mechanical strength of a thin-film membrane.

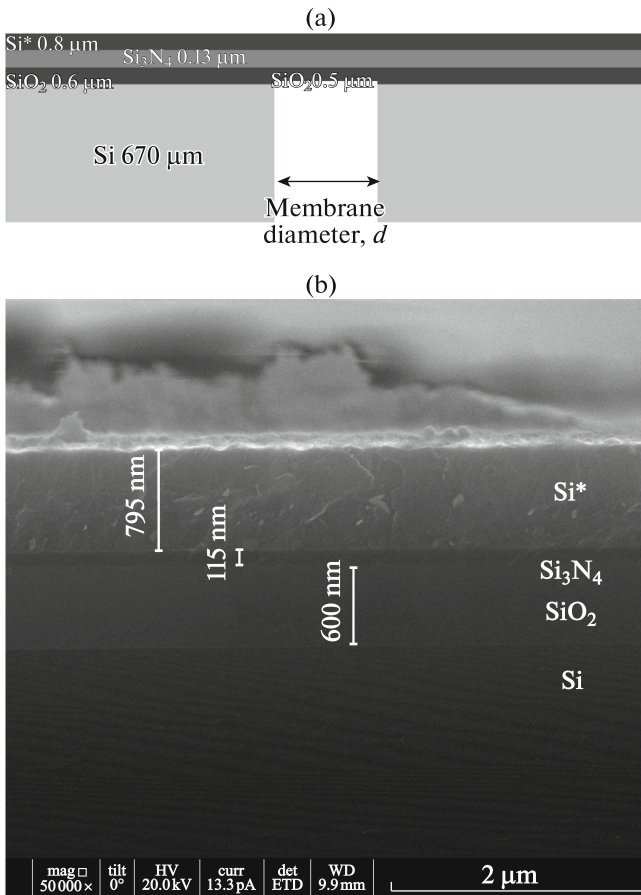

Fig. 2. Analyzed structure: (a) general view; (b) cut of the structure in the thin film region.

face. The circular shape ensures much lower values of elastic strains as compared to the rectangular shape of membranes. The strains are distributed uniformly over the membrane contour and in the membrane material [8]. There is also a method for increasing mechanical strength, which involves a change in the stoichiometric ratio of atoms in the material (e.g., by increasing the carbon concentration in SiC) [9]. Other factors facilitating the increase in mechanical strength include the decrease in the number of surface defects [10], the change in the grain size in the structure [11], and doping of the film material with copper, zinc, magnesium, manganese, and silicon atoms [5].

1. STRUCTURE PREPARATION

We used a KDB12 silicon monocrystalline wafer with a diameter of 150 mm with the (100) crystallographic orientation and a thickness of 670 μm. A circular membrane was formed on a square Si crystal with a side of 6 mm. The membrane structure under investigation consists of the upper polycrystalline silicon layer with a thickness of 0.8 ± 0.05 μm, a silicon nitride layer with a thickness of 0.13 ± 0.02 μm, and a lower dielectric silicon oxide layer with a thickness of 0.5 ± 0.1 μm (Fig. 2). The topology of the set of membranes is a circle with a diameter of 0.25 mm located at the center of the crystal. The membrane does not contain mechanical stress concentrators because of the application of a circular etching template.

2. ANALYSIS OF MECHANICAL STRENGTH OF THE STRUCTURE

The range of mechanical strength values for silicon oxide film was given in the following publications: from 1.2 to 1.9 GPa for PECVD silicon oxide [12], 0.364 ± 0.057 GPa for PECVD SiO_2 of thickness 1.0 μm [13], 0.89 ± 0.07 GPa for thermal SiO_2 layers of thickness from 507 to 985 nm [14], and 8.4 GPa for filamentary SiO_2 structures [15]. The mechanical strength of a silicon nitride film is 14.0 GPa [15–17]. It was noted in monograph [18] that the mechanical strength of the silicon nitride film obtained by the LPCVD method varies in the range from 10.8 to 11.7 GPa for a film thickness from 72.6 to 83.4 nm. According to the results obtained in [19], the mechanical strength of LPCVD silicon nitride is 5.87 GPa. In an analysis of the literature, we came across the following values of the mechanical strength of thin layers of polycrystalline silicon: from 1.8 to 3.7 GPa depending on the grain size [20], 8.11 ± 0.31 GPa [21], 1.7 ± 0.5 GPa for a surface area of 225 μm^2, 1.3 ± 0.3 GPa for 1100 μm^2 and 0.6 ± 0.2 GPa for 8600 μm^2 [22], 1.0–1.2 GPa [23], 3.15 ± 0.69 GPa [24], 0.8–1.1 GPa [25], and 1.0–1.5 GPa [26]. For further calculations, we used the mechanical strength of 1.8 GPa for polycrystalline silicon, 0.365 GPa for silicon oxide, and 14 GPa for silicon nitride.

The theoretical value of mechanical strength (maximal mechanical stresses) σ_t of a membrane is calculated by the formula

$$\sigma_t = \frac{\sigma_{PolySi} h_{PolySi} + \sigma_{SiO_2} h_{SiO_2} + \sigma_{Si_3N_4} h_{Si_3N_4}}{h_{PolySi} + h_{SiO_2} + h_{Si_3N_4}}, \quad (1)$$

where h_{PolySi} is the thickness of the polycrystalline silicon layer, h_{SiO_2} is the thickness of the silicon oxide layer, and $h_{Si_3N_4}$ is the thickness of the silicon nitride layer.

The calculated value of σ_t is 3.2 GPa. The mechanical stress distribution over the membrane diameter is calculated using the formula [5]

$$\sigma = \frac{3P}{8h^2}\sqrt{((1+\mu)^2(2a^4 - 8a^2r^2) + r^4(10 + 12\mu + 10\mu^2))}, \quad (2)$$

where a is the membrane radius, h is the membrane thickness, P is the pressure on the membrane, μ is the Poisson ratio of the membrane, and r is the distance from the membrane center.

Figure 3a shows the results of calculations based on formula (2) for the mechanical stress distribution over

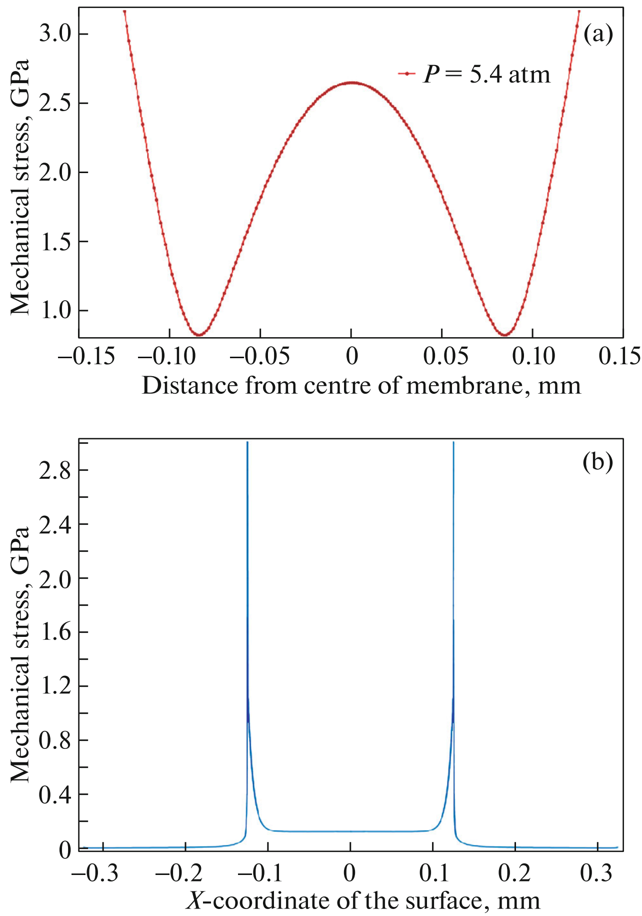

Fig. 3. Distribution of mechanical stresses in a membrane with a diameter of 0.25 mm: (a) calculated by formula (4) for $P = 5.4$ atm; (b) simulation for $P = 5.4$ atm.

the membrane diameter. According to analytic calculation, maximal mechanical stresses σ_{max} appear when the distance from the center (middle) of the membrane equals its radius (i.e., $r = a$). Therefore, the predicted critical excess pressure P_{cr} is calculated by the following formula [5]:

$$P_{cr} = \frac{\sigma_{max} h^2}{a^2 B(\mu)}. \quad (3)$$

Coefficient $B(\mu)$ is calculated as $\frac{3}{4}\sqrt{1+\mu^2}$. Poisson ratio P_{cr} of the membrane is calculated using an approach analogous to formula (1). Taking it into account that $\mu_{PolySi} = 0.22$, $\mu_{SiO_2} = 0.2$, and $\mu_{Si_3N_4} = 0.23$, the Poisson ratio for the membrane is 0.21. Consequently, the value of coefficient $B(\mu)$ is 0.76. Therefore, according to calculations based on formula (2), the predicted value of critical excess pressure P_{cr} for a membrane with a diameter of 0.25 mm is 0.554 MPa.

We have also constructed a model in the Comsol Multiphysics medium. The coordinates of the sub-

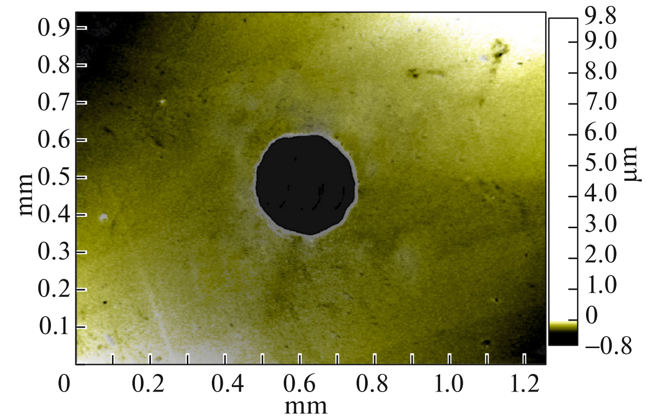

Fig. 4. Top view of the structure after rupture.

strate region along the X axis are from –325 to –125 μm and from 125 to 325 μm. The membrane region is located symmetrically relative coordinate $X = 0$. We choose a rectangular mesh in the membrane region, which contained 1040 elements along the X axis and 22 elements along the Y axis (each layer of the film was split into ten elements, while the Si_3N_4 layer contained two cells because of its small thickness). In the silicon substrate region, we chose a free triangular type of the mesh. We obtained the dependence of the mechanical stress distribution in a membrane with a diameter of 0.25 mm and in a thin film under an excess pressure of 0.54 MPa (Fig. 3b) according to experimental data. The form of the stress distribution in the membrane region coincides with the data of earlier publication [4].

The mechanical stress maximum is localized at the membrane/substrate interface. The model developed in the Comsol medium correlates well (with a relative error of 0.25%) with experimental and theoretical data because the maximal value of mechanical stresses is 3.17 GPa for an excess pressure of 0.54 MPa. In the image of the structure after critical deformation of the membrane (Fig. 4), the membrane material is not detected in the silicon cavity. Therefore, the membrane is ruptured over the membrane/substrate interface.

3. ANALYSIS OF THE BIAXIAL ELASTIC MODULUS OF THE STRUCTURE

Analyzing the dependence of membrane deflection w as a function of excess pressure P,

$$P = C_1 \frac{\sigma_0 h w}{a^2} + C_2 \frac{E h w^3}{(1-\mu)a^4}, \quad (4)$$

where P is the excess pressure, σ_0 are the residual mechanical stresses in the structure for $P = 0$, h is the membrane thickness, w is the value of membrane deflection, a is the membrane radius, E is the Young

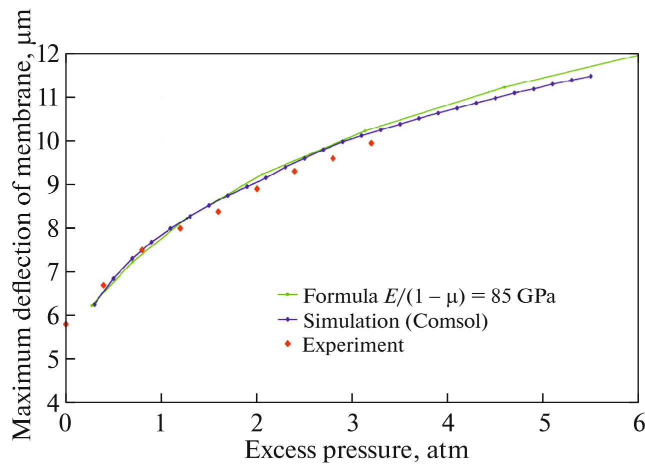

Fig. 5. Dependence of the maximal deflection of the membrane on the excess pressure for a diameter of 0.25 mm.

modulus, and μ is the Poisson ratio, we can determine biaxial elastic modulus $E/(1-\mu)$.

The values of coefficients C_1 and C_2 depend on the membrane shape. Usually, for operation with circular membranes, the values of $C_1 = 4$ and $C_2 = 8/3$ are used. The $P(w)$ dependence can be divided into the steep and flat segments. The criterion for the steep segment holds for small values of membrane deflection w; i.e., the first term is much larger than the second one. The value of biaxial elastic modulus $E/(1-\mu)$ is calculated on the flat segment of dependence (4) for large values of membrane deflection w (i.e., the first term in (4) can be omitted):

$$\frac{E}{1-\mu} = \frac{Pa^4}{C_0 h w^3}. \quad (5)$$

The Young modulus is 225 GPa for silicon nitride [19], 60.1 ± 3.4 GPa for silicon oxide [13], and 155 GPa for polycrystalline silicon [16, 20]. Consequently, the Young modulus of the membrane is 128 GPa. The theoretical value of biaxial elastic modulus $E/(1-\mu)$ of the membrane is 162 GPa for Poisson ratio $\mu = 0.21$ for the membrane, which was calculated earlier.

The dependence of the maximal deflection of the membrane on the excess pressure is shown in Fig. 5. The value of residual stresses of the structure calculated using formula (4) is 100 MPa. To improve the correlation between the result of calculation based on formula (4), simulation in the Comsol medium, and experimental data, the initial deflection (for $P = 0$) is taken as 4.5 μm for simulation and in the analytic calculation, and biaxial elastic modulus $E/(1-\mu)$ is 85 GPa.

Based on Fig. 5, we can draw several conclusions. The relative error in the formula with experimental data is 3.24%, while the relative error of simulation with experimental data is 3.02%. The initial structure has a considerable deflection of the membrane, which is not accounted in the initial formula and in the Comsol model. Calculating the elastic modulus by formula (5) from experimental data at pressure $P = 0.32$ MPa, we obtain 20 GPa, which is several times smaller than the theoretical value. This can be due to the fact that the experimentally determined array of values of $w(P)$ lies in the steep segment of dependence (4). Consequently, it is necessary to develop accessories for protecting the profilometer from the material of exploding membrane during scanning. This will give a larger data array for $w(P)$, which will improve the accuracy in the determination of the biaxial elastic modulus.

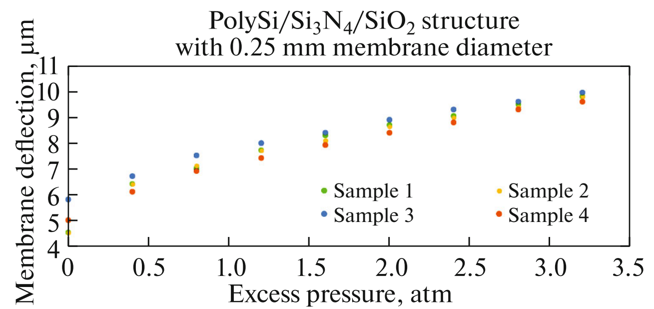

Fig. 6. Experimental dependence of the membrane deflection on the excess pressure.

4. EXPERIMENTAL DETERMINATION OF MECHANICAL STRENGTH

For determining mechanical properties of membrane elements, we modified the stand designed earlier in [5]. The excess pressure is now fed from the mains (and not from a compressor). This permitted to extend the upper limit of pressure to 0.65 MPa and improved the stability of pressure value in the system.

We determined experimentally the values of the critical excess pressure on the modernized stand. For a diameter of 0.25 mm, the mechanical strength of the $PolySi/Si_3N_4/SiO_2$ membrane with a diameter of 0.25 mm is 0.52 ± 0.04 MPa (15 samples). It can be seen that our result are characterized by high reproducibility. The experimental value of mechanical strength of a three-layer membrane is 3.13 GPa.

In experiments with excess pressures higher than 0.32 MPa, the membrane deflection was not measured (Fig. 6). This limitation is due to protection of the costly objective of the profilometer from the material of the exploding membrane. Its rupture can occur during scanning of the sample surface by the profilometer.

CONCLUSIONS

The experimental value of the mechanical strength of a three-layer $PolySi/Si_3N_4/SiO_2$ membrane is

3.13 GPa, the biaxial elastic modulus $E/(1 - \mu)$ amounts to 20 GPa. The critical excess pressure of the $PolySi/Si_3N_4/SiO_2$ membrane structures on a silicon substrate is 0.52 ± 0.04 MPa for a diameter of 0.25 mm. These results make it possible to use such membranes as anodes of shooting X-ray sources with a high mechanical strength safety margin. The increase in mechanical strength is achieved by using a set of layers instead of a monolayer membrane and the effect of increase in the film strength by modernization of deposition technology.

FUNDING

The research work was performed on the equipment of the Microsystem Technology and Electronic Component Base Center for Collective Use of National Research University "MIET" with the support of the Ministry of Education and Science of the Russian Federation, state contract no. 14.581.21.0021, UN RFMEFI58117X0021.

CONFLICT OF INTEREST

The authors declare that they have no conflicts of interest.

REFERENCES

1. N. A. Dyuzhev, G. D. Demin, A. E. Pestov, N. N. Salashchenko, and N. I. Chkhalo, *Microelectronics-2019*, p. 429.
2. B. Wu and A. Kumar, Appl. Phys. Rev. **1** (1), 011104 (2014). https://doi.org/10.1063/1.4863412
3. N. I. Chkhalo, A. Ya. Lopatin, A. E. Pestov, N. N. Malashchenko, G. D. Demin, N. A. Dyuzhev, and M. A. Makhiboroda, Proc. SPIE **11022**, 110221M (2019). https://doi.org/10.1117/12.2522105
4. V. V. Shpejzman, V. I. Nikolaev, A. O. Pozdnyakov, A. V. Bobyl', R. B. Timashov, and A. I. Averkin, Tech. Phys. **90** (1), 79 (2020). https://doi.org/10.21883/JTF.2020.01.48665.148-19]
5. E. E. Gusev, A. V. Borisova, A. A. Dedkova, A. A. Salnikov, and V. Y. Kireev, IEEE Conf. of Russian Young Researchers in Electrical and Electronic Engineering (EIConRus) (St. Petersburg—Moscow, Russia, January 28–31, 2019), No. 8657243, pp. 1990–1994. https://doi.org/10.1109/eiconrus.2019.8657243
6. A. S. Savinykh, G. I. Kanel, and S. V. Razorenov, Tech. Phys. **55** (6), 839 (2010). https://doi.org/10.1134/S1063784210060150
7. Yu. V. Zhilyaev, S. D. Raevskii, D. Z. Grabko, D. S. Leu, M. E. Kompan, S. A. Yusupova, and M. P. Shcheglov, Tech. Phys. Lett. **31** (5), 367 (2005). https://doi.org/10.1134/1.1931770
8. A. I. Vlasov, T.A. Tsivinskaya, and V.A. Shakhnov, *Proc. 7th All-Russia Sci. & Technol. Conf. "Problems of Advanced Micro- and Nanoelectronic Systems Development" (MES-2016)* (Zelenograd, Russia, October 3–7, 2016). http://www.mes-conference.ru/data/year-2016/pdf/D084.pdf.
9. S. L. Shikunov and V. N. Kurlov, Tech. Phys. **62** (12), 1869 (2017). https://doi.org/10.1134/S1063784217120222
10. M. G. Mueller, M. Fornabaio, G. Zagar, and A. Mortensen, Acta Mater. **105**, 165 (2016). https://doi.org/10.1016/j.actamat.2015.12.006
11. R. Venkatraman and J. C. Bravman, J. Mater. Res. **7** (8), 2040 (1992). https://doi.org/10.1557/JMR.1992.2040
12. T. Tsuchiya, A. Inoue, and J. Sakata, Sens. Actuators, A **82** (1–3), 286 (2000). https://doi.org/10.1016/S0924-4247(99)00363-5
13. W. N. Sharpe, J. Pulskamp, D. S. Gianola, C. Eberl, R.G. Polcawich, and R. J. Thompson, Exp. Mech. **47**, 649 (2007). https://doi.org/10.1007/s11340-006-9010-z
14. Jinling Yang, A. Gaspar, and O. Paul, J. Microelectromech. Syst. **17** (5), 1120 (2008). https://doi.org/10.1109/JMEMS.2008.928706
15. K. Petersen, Proc. IEEE **70** (5), 420 (1982).
16. Tai-Ran Hsu, *MEMS and Microsystems: Design and Manufacture* (McGraw-Hill Education, Boston, 2002).
17. M. Madou, *Fundamentals of Microfabrication* (Taylor & Francis, London, 1997).
18. Qing An Huang, *Micro Electro Mechanical Systems* (Springer, Singapore, 2018).
19. R. L. Edwards, G. Coles, and W. N. Sharpe, Exp. Mech. **44** (1), 49 (2004). https://doi.org/10.1007/bf02427976
20. T. Tsuchiya, J. Sakata, and Y. Taga, MRS Online Proc. Libr. **505**, 285 (1998). https://doi.org/10.1557/proc-505-285
21. T. Ozaki, T. Koga, N. Fujitsuka, H. Makino, H. Hohjo, and H. Kadoura, Sens. Actuators, A **278**, 48 (2018). https://doi.org/10.1016/j.sna.2018.05.034
22. R. Vayrette, J.-P. Raskin, and T. Pardoen, Eng. Fract. Mech. **150**, 222 (2015).
23. B. L. Boyce, J. M. Grazier, T. E. Buchheit, and M. J. Shaw, J. Microelectromech. Syst. **16** (2), 179 (2007).
24. B. Kaiser, C. Drabe, T. Graßhoff, H. Conrad, and H. Schenk, J. Micromech. Microeng. **25** (8), 085003 (2015). https://doi.org/10.1088/0960-1317/25/8/085003
25. W. N. Sharpe and J. Bagdahn, Mech. Mater. **36** (1–2), 3 (2004). https://doi.org/10.1016/s0167-6636(03)00027-9
26. W. N. Sharpe and K. T. Turner, *Proc.7th Int. Fatigue Congr. (Fatigue'99), Beijing, China, June 8–12, 1999* (Higher Education, Beijing, 1999), pp. 1837–1844.

Translated by N. Wadhwa